

Thermodynamics of quantum Heisenberg spin chains

Tao Xiang

*Research Centre in Superconductivity, University of Cambridge, Madingley Road, Cambridge CH3 0HE, United Kingdom
and Institute of Theoretical Physics, Academia Sinica, P.O. Box 2735, Beijing 100080, China*

(Received 23 April 1998)

Thermodynamic properties of the quantum Heisenberg spin chains with $S=1/2$, 1, and $3/2$ are investigated using the transfer-matrix renormalization-group method. The temperature dependence of the magnetization, susceptibility, specific heat, spin-spin correlation length, and several other physical quantities in a zero or finite applied field are calculated and compared. Our data agree well with the Bethe ansatz, exact diagonalization, and quantum Monte Carlo results and provide further insight into the quantum effects in the antiferromagnetic Heisenberg spin chains. [S0163-1829(98)00838-8]

I. INTRODUCTION

There are a lot of quasi-one-dimensional compounds whose behaviors can be adequately described within the framework of interacting spin chains governed by the Heisenberg model. Extensive studies on this model have shed light on the quantum nature of spin dynamics. In 1983, Haldane predicted that the one-dimensional (1D) Heisenberg antiferromagnetic model with integer spin has an excitation gap and a finite correlation length.¹ Since then a great amount of experimental and theoretical effort has been made towards understanding the difference between half-integer and integer spin chains.

In this paper we report results of a transfer-matrix renormalization-group²⁻⁴ (TMRG) study for the thermodynamics of quantum Heisenberg spin chains. We have calculated the magnetic susceptibility, specific heat, spin-spin correlation length, and other experimentally relevant quantities as functions of temperature and applied magnetic field for the $S=1/2$, 1, and $3/2$ spin chains.

The Heisenberg model is defined by the Hamiltonian

$$\hat{H} = \sum_i^N h_i, \quad h_i = JS_i \cdot S_{i+1} - \frac{H}{2}(S_{iz} + S_{i+1z}), \quad (1)$$

where J is the spin exchange constant and H is an applied magnetic field.⁵ In this paper we consider antiferromagnetic spin chains only. We use units in which $J=1$.

The spin-1/2 Heisenberg model is integrable by Bethe ansatz. Many of its thermodynamic quantities, for example, the specific heat and the spin susceptibility, can be calculated by solving the Bethe ansatz equations. The conformal field theory is also very useful in analyzing the low-temperature low-field thermodynamic properties, since the $S=1/2$ Heisenberg model is equivalent to the $k=1$ Wess-Zumino-Witten nonlinear σ model.

Higher spin Heisenberg models are not at present amenable to rigorous solution. The finite-temperature properties of the model were studied mainly through transfer-matrix,⁶ quantum Monte Carlo,⁷⁻⁹ and other approximate methods.^{10,11}

At zero field, the ground state of \hat{H} is a spin singlet with zero spin magnetization. At finite field, the magnetization of the ground state becomes finite and increases with increasing H . There is a critical field H_{c2} beyond which all spins are

fully polarized at zero temperature. If we denote $E(N, S)$ as the lowest eigenvalue of an N -site Heisenberg chain with total spin S at $H=0$, then it is straightforward to show that $H_{c2} = E(N, S_{\max}) - E(N, S_{\max} - 1) = 4S$, independent of N . Below H_{c2} , a canted Néel order, namely, a state which has both ferromagnetic order along the z axis and antiferromagnetic order in the xy plane, exists at sufficiently low temperature, and the pitch vector (i.e., the value of the momenta at which the static structure factor shows a peak) decreases continuously from π to 0 with increasing H .

Integer spin chains can be described by the quantum nonlinear σ model. It is from the study of this model that Haldane made the famous ‘‘Haldane conjecture.’’ The ground state of the $O(3)$ σ model has a finite excitation gap and consequently a finite correlation length. The application of a magnetic field causes a Zeeman splitting of the triplet with one member crossing the ground state at a critical field H_{c1} whose value is equal to the excitation gap Δ . When $H < H_{c1}$, the Haldane gap persists and the ground state is still a nondegenerate spin singlet state. When $H_{c1} < H < H_{c2}$, the ground state has a nonzero magnetization with gapless excitations. Thus across H_{c1} , an integer spin system undergoes a commensurate to incommensurate transition. This is an interesting feature which is absent in a half-odd-integer spin system. Evidence for such transitions has been used to identify the Haldane gap in NENP (Ref. 12) and other quasi-1D spin compounds.¹³ Just above H_{c1} , the ground state can be regarded as a Bose condensate of the low-energy boson. Varying the magnetic field is equivalent to varying the chemical potential for this boson and the (uniform) magnetization corresponds to the boson number.¹⁴

II. TMRG

In this section we briefly discuss the TMRG method. A more detailed introduction to the method can be found in Refs. 3 and 4.

The TMRG method starts by mapping a 1D quantum system onto a 2D classical one with the Trotter-Suzuki decomposition and represents the partition function as a trace of a power function of virtual transfer matrix T_M :

$$Z = \text{Tr} e^{-\beta H} = \lim_{M \rightarrow \infty} \text{Tr} T_M^{N/2}, \quad (2)$$

where M is the Trotter number. T_M is defined by an inner product of $2M$ local transfer matrices

$$\begin{aligned} & \langle \sigma_3^1, \dots, \sigma_3^{2M} | T_M | \sigma_1^1, \dots, \sigma_1^{2M} \rangle \\ &= \sum_{\{\sigma_2^k\}} \prod_{k=1}^M t(\sigma_3^{2k-1} \sigma_3^{2k} | \sigma_2^{2k-1} \sigma_2^{2k}) \\ & \quad \times t(\sigma_2^{2k} \sigma_2^{2k+1} | \sigma_1^{2k} \sigma_1^{2k+1}), \end{aligned}$$

where

$$t(\sigma_{i+1}^k \sigma_{i+1}^{k+1} | \sigma_i^k \sigma_i^{k+1}) = \langle -\sigma_i^{k+1}, \sigma_{i+1}^{k+1} | e^{-\tau h_i} | \sigma_i^k, -\sigma_{i+1}^k \rangle$$

and $\tau = \beta/M$. $|\sigma_i^k\rangle$ is an eigenstate of S_i^z and σ_i^k is the corresponding eigenvalue: $S_i^z |\sigma_i^k\rangle = \sigma_i^k |\sigma_i^k\rangle$. The superscripts and subscripts in T_M and t represent the spin positions in the Trotter and real space, respectively.

T_M conserves the total spin in the Trotter space, i.e., $\sum_k \sigma_i^k$. Thus T_M is block diagonal according to the value of $\sum_k \sigma_i^k$.⁴ For the $S=1/2$ Heisenberg model, it was shown rigorously that the maximum eigenstate of T_M is nondegenerate and in the $\sum_k \sigma_i^k = 0$ subspace, irrespective of the sign of J and the value of H .¹⁵ When $S > 1/2$, we found numerically that the maximum eigenvectors of T_M are also in the $\sum_k \sigma_i^k = 0$ subblock.

In the thermodynamic limit, the free energy per spin is given by

$$F = - \lim_{N \rightarrow \infty} \frac{1}{N\beta} \ln Z = - \frac{1}{2\beta} \lim_{M \rightarrow \infty} \ln \lambda_{\max}, \quad (3)$$

where λ_{\max} is the maximum eigenvalue of T_M . From the derivatives of F one can in principle calculate all thermodynamic quantities. The internal energy U and the spin magnetization M_z could, for example, be calculated from the first derivative of F with respect to H and T , respectively. However, numerically it is better to calculate U and M_z directly from the eigenvectors of T_M .⁴ The spin susceptibility $\chi = \partial M_z / \partial H$ and the specific heat $C = \partial U / \partial T$ can then be calculated by numerical derivatives. The specific heat so determined is generally found to be less accurate than, for example, the susceptibility data at low T . The reason for this is that U changes very slowly with T (or equivalently C is very small) at low T , and a small error in U would lead to a relatively large error in C .

The correlation length of the spin-spin correlation functions, defined by $\xi_\alpha^{-1} = -\lim_{L \rightarrow \infty} \ln \langle S_{i,\alpha} S_{i+L,\alpha} \rangle$, can also be calculated from this method. The longitudinal and transverse correlation lengths are determined by

$$\xi_z^{-1} = \frac{1}{2} \lim_{M \rightarrow \infty} \ln \frac{\lambda_{\max}}{\lambda_2}, \quad (4)$$

$$\xi_x^{-1} = \frac{1}{2} \lim_{M \rightarrow \infty} \ln \frac{\lambda_{\max}}{\lambda_1}, \quad (5)$$

where λ_2 is the second largest eigenvalue of T_M in the subspace $\sum_k \sigma_k^i = 0$ and λ_1 is the largest eigenvalue of T_M in the subspace $\sum_k \sigma_k^i = \pm 1$.

Figure 1 shows the configuration of superblock used in

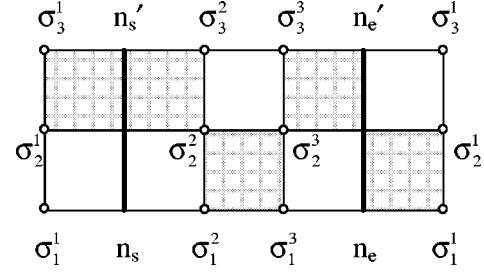


FIG. 1. A pictorial representation of a superblock, which consists of system and environment blocks connected by three added spins to form a periodic chain. n_s and n_e are indices for the system and environment blocks, respectively. Initially the system block contains two spins and the environment block contains only one spin. At each iteration the system and environment blocks are augmented by adding σ^1 to each of the blocks. The augmented system \tilde{n}_s is formed by $n_s \oplus \sigma^1$, and the augmented environment \tilde{n}_e is formed by $\sigma^1 \oplus n_s$.

our calculation. This configuration of superblock is different from those used in Refs. 3 and 4. The advantage for forming the superblock in such a way is that the transfer matrix T_M in this case can always be factorized as a product of two sparse matrices (which are block diagonal with respect to n_s and $\sigma_3 \otimes n_e$, respectively). To treat these two sparse matrices instead of T_M itself allows us to save both computer memory space and CPU time.

We compute the maximum eigenvalue λ_{\max} and the corresponding right and left eigenvectors $|\psi^R\rangle$ and $\langle\psi^L|$ of T_M using an implicitly restarted Arnoldi method.¹⁶ This method is more efficient than the power method which we used before.^{3,4} $\lambda_{1,2}$ can also be calculated from this method, but their truncation errors are generally larger than those of λ_{\max} . Thus the correlation lengths determined from Eqs. (4) and (5) are generally expected to be less accurate than the free energy or other thermodynamic quantities.

In the TMRG method, the density matrix for the augmented system or environment block is nonsymmetric, which is different than in the zero-temperature density-matrix renormalization-group (DMRG) method. Numerically it is much more difficult to treat accurately a nonsymmetric matrix than a symmetric one because the errors in $|\psi^R\rangle$ and $\langle\psi^L|$ may affect the (semi) positiveness of the density matrix and increase the truncation error of the TMRG.

The TMRG treats directly an infinity spin chain. There is therefore no finite size effect. The error caused by the finiteness of the Trotter number (or τ) is of order τ^2 , which is generally very small. The error resulting from the truncation of basis states is difficult to estimate. A rough estimation for this type of error can be obtained from the value of truncation error, which is smaller than 10^{-3} in all our calculations. More accurate results can be obtained simply by extrapolating the results with respect to both τ and the number m of states retained.

III. RESULTS

A. $S=1/2$

The $S=1/2$ Heisenberg model is by far the best understood spin system. In the absence of field, the ground state is

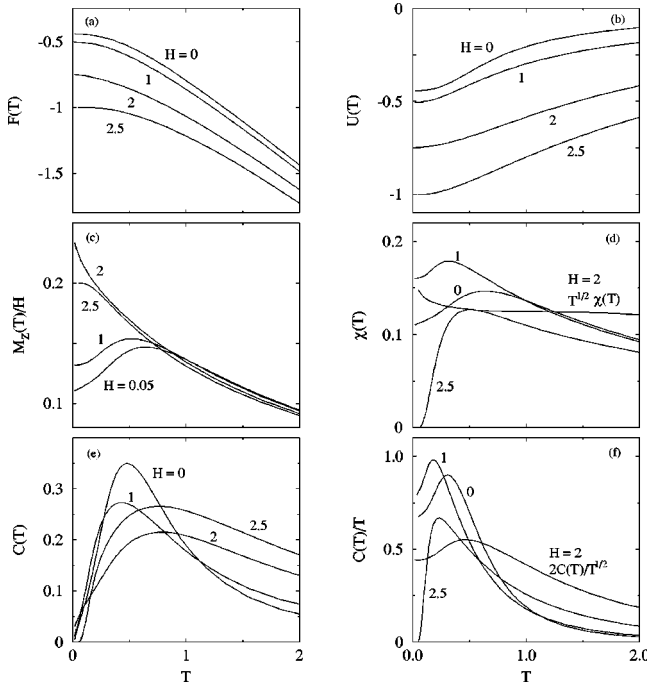


FIG. 2. (a) Free energy $F(T)$, (b) internal energy $U(T)$, (c) ratio between the magnetization $M_z(T)$ and the field H , (d) spin susceptibility $\chi(T)$, (e) specific heat $C(T)$, and (f) $C(T)/T$, per lattice site, for the spin-1/2 Heisenberg model in four applied fields, $H=0$ (or 0.05), 1, 2, and 2.5. When $H=2$, $T^{1/2}\chi(T)$ and $2C(T)/T^{1/2}$, instead of $\chi(T)$ and $C(T)/T$, are shown in (d) and (f), respectively. $\tau=0.1$ and $m=81$ are used in the TMRG calculations.

massless and the Bethe ansatz result for the ground state energy is $(1/4 - \ln 2)$. The lowest excitations states are spin triplets with a spin wave spectrum¹⁷ $\varepsilon(k) = (\pi/2)|\sin k|$. Above this lower boundary of excitations, there is a two-parameter continuum of spin wave excitations with an upper boundary given by¹⁸ $\varepsilon(k) = \pi|\sin(k/2)|$. There are other excitations above this upper boundary.

The specific heat of the model was first calculated numerically by Bonner and Fisher.¹⁹ They found that at low temperature $C \sim 0.7T$ when $H=0$. Later, Affleck,²⁰ using the conformal field theory, found that $C = (2/3)T$. The zero-field zero-temperature magnetic susceptibility is $\chi = 1/\pi^2$. This result was obtained by Griffiths with the Bethe ansatz and numerics.²¹ Recently, Eggert, Affleck, and Takahashi²² found that the zero-field susceptibility approaches its zero-temperature value logarithmically when $T < 0.01$,

$$\chi = \frac{1}{2\pi v} \left[1 + \left(2 \ln \frac{T_0}{T} \right)^{-1} \right], \quad (6)$$

where $v = (\pi/2)$ is the spin wave velocity and $T_0 \approx 7.7$.

Figure 2 shows the TMRG results for a number of thermodynamic quantities of the $S=1/2$ antiferromagnetic Heisenberg model in various magnetic fields with $m=81$ and $\tau=0.1$. At zero field, the TMRG reproduces accurately the results which were previously obtained by the Bethe ansatz or conformal field theory. The extrapolated zero-field zero-temperature values of the internal energy $U(T)$ (i.e., ground state energy), the spin susceptibility $\chi(T)$, and the linear coefficient of the specific heat $C(T)$, are -0.443 , 0.109 , and

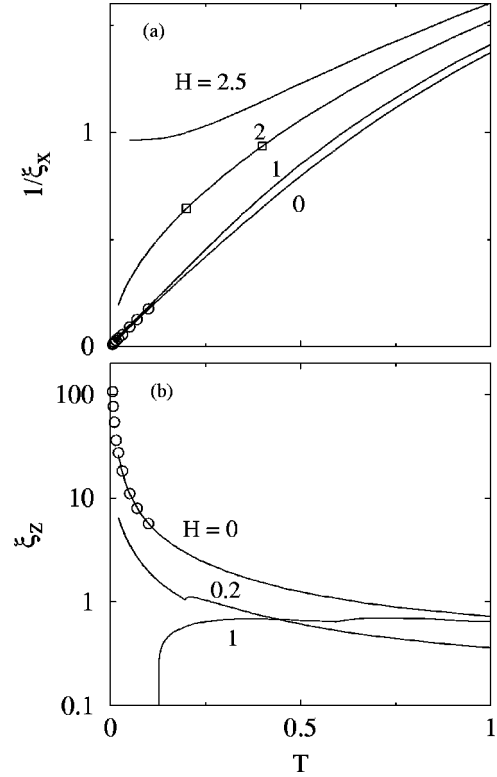


FIG. 3. (a) $1/\xi_x$ and (b) ξ_z vs T for the spin-1/2 Heisenberg models. $\tau=0.1$ and $m=81$ are used in the TMRG calculations. The circles (Ref. 23) and squares (Ref. 24) are thermal Bethe ansatz results.

0.66 , respectively. In all the fields which we studied, the peak position of $\chi(T)$ is located at a temperature which is about twice the peak temperature of $C(T)/T$. This is due to the fact that $\chi(T)$ is a measure of two-particle excitations and $C(T)/T$ is only a measure of one-particle density of states. The maximum of χ when $H=0$ is approximately equal to 0.147 at $T=0.64$, consistent with the Bethe ansatz calculation.²²

There is a significant change in the temperature dependences of χ and C when H is below and above a critical field $H_{c2}=2$. Below H_{c2} , both C/T and χ are finite at zero temperature, which shows that gapless spin excitations with a finite low-energy density of states exist in this regime. When $H=H_{c2}$, both χ and C/T vary as $1/\sqrt{T}$ at low temperature; the extrapolated values of $\sqrt{T}\chi$ and C/\sqrt{T} at zero temperature are 0.152 and 0.22 , respectively. The divergency of χ and C/T at $T=0$ implies that the density of states of spin excitations is divergent at zero energy when $H=H_{c2}$. Above H_{c2} , there is a gap in the excitation spectrum as both χ and C/T drop to zero exponentially at low temperatures. The value of the gap estimated from the low-temperature behavior of χ and C grows linearly with $H-H_{c2}$.

Figure 3 shows the longitudinal and transverse correlation lengths of the $S=1/2$ model in different applied fields. When $H=0$, $\xi_x = \xi_z$ diverges at zero temperature and the slope of ξ_z^{-1} at low temperature is approximately equal to 2, in agreement with the thermal Bethe ansatz as well as the $k=1$ WZW σ model result²³

$$\xi_z^{-1} = T \left[2 - \left(\ln \frac{T_0}{T} \right)^{-1} \right]. \quad (7)$$

In the presence of magnetic field, ξ_z is substantially suppressed and becomes finite at zero temperature. As the correlation length is inversely proportional to the energy gap of excitations, the finiteness of ξ_z at $T=0$ means that the longitudinal spin excitation modes are massive in a field. There is a small dip in the curve of ξ_z at $T\sim 0.4$ when $H=0.2$ or at $T\sim 0.6$ when $H=1$. This dip feature of ξ_z , as will be shown later, appears also in large S systems.

The effect of the applied field on the transverse spin excitation modes is weaker than the longitudinal modes. The transverse spin excitations become massive only when $H > H_{c2}$. Below H_{c2} , ξ_x drops to zero linearly with T , as for the case $H=0$. When $H=H_{c2}$, ξ_x drops to zero as \sqrt{T} . Clearly the thermodynamics of the Heisenberg model in a field is mainly determined by the transverse excitation modes at low temperatures.

A simple understanding of the above results can be obtained from an equivalent spinless fermion model of the $S=1/2$ Heisenberg model:

$$\hat{H} = \sum_i \left[-\frac{1}{2}(c_{i+1}^\dagger c_i + c_i^\dagger c_{i+1}) + (H-1)c_i^\dagger c_i + \left(\frac{1}{4} - H\right) + c_i^\dagger c_i c_{i+1}^\dagger c_{i+1} \right], \quad (8)$$

where c_i is a spinless fermion operator which is linked to the $S=1/2$ spin operator by the Jordan-Wigner transformation $c_i = S_i^+ \exp(i\pi \sum_{l<i} c_l^\dagger c_l)$. The magnetic field is equivalent to a chemical potential for the fermions. When $H=0$, the ground state has zero uniform magnetization, corresponding to a half filled fermion band. As H increases, the ground state is ferromagnetically polarized and the Fermi energy shifts down. When H is smaller than the critical field H_{c2} , the ground state of this fermion model has no gap but the spin orientation is canted, i.e., in an incommensurate state. The pitch angle of this incommensurate ground state, namely, the wave vector at which the maximum of the spin-spin correlation function appears, can be estimated from the Fermi momentum of noninteracting fermions as $2k_F = [1 - 2M_z(H)]\pi$. This value of k_F is not normalized by interactions according to the Luttinger theorem.

Above H_{c2} , there are no fermions at the ground state. At low temperature, the number of fermions excited from the ground state is small. Thus, as a good approximation, the interaction term in Eq. (8) can be ignored at low temperatures. For the noninteracting system, the energy dispersion of fermion excitations from the ground state is given by $\varepsilon_k = H - (1 + \cos k)$, which has a gap of $H - H_{c2}$. When $H = H_{c2}$, $\varepsilon_k = (1 - \cos k)$, the density of states of excited fermions varies as $1/\sqrt{\varepsilon}$ at low energy. From the standard theory of noninteracting fermions, it is straightforward to show that this singular density of states will cause both χ and C/T to diverge as $1/\sqrt{T}$ at low temperature. When $H > H_{c2}$, there is a gap in the fermion excitations, and both χ and C should decrease exponentially at low temperature. These results are just what we found in Fig. 2.

B. $S=1$

As mentioned previously, there are two critical fields in the spin-1 Heisenberg model, H_{c1} and H_{c2} : below H_{c1} , the

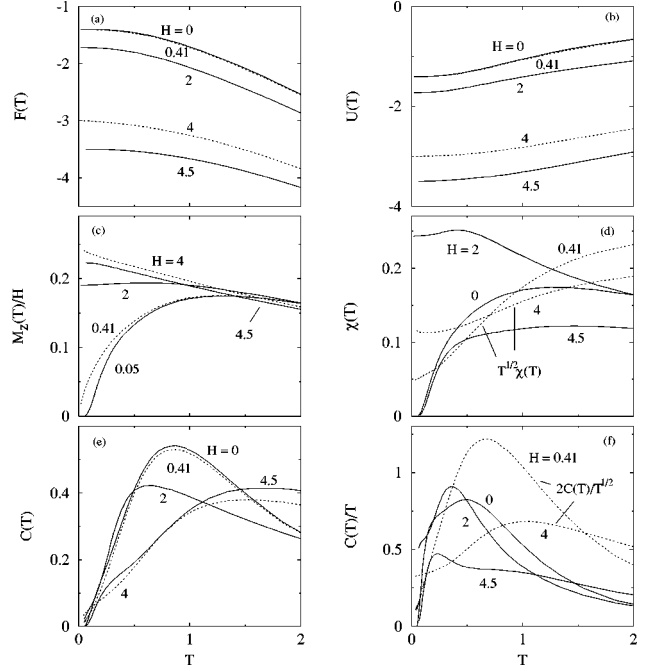


FIG. 4. Thermodynamic quantities for the spin-1 Heisenberg model in five applied fields, $H=0$ (or 0.05), 0.4105, 2, 4, and 4.5. When $H=0$ and 0.4105, $F(T)$ and $U(T)$ are almost indistinguishable in the figure. When $H=0.4105$ or 4, $T^{1/2}\chi(T)$ and $2C(T)/T^{1/2}$ (dotted lines) are shown in (d) and (f), respectively. $\tau=0.1$ and $m=100$ are used in the TMRG calculations.

ground state is a massive spin singlet; above H_{c2} , the ground state becomes a fully polarized ferromagnetic state; between H_{c1} and H_{c2} , the ground state is massless and has a finite magnetization. The temperature dependence of thermodynamic quantities of the $S=1$ model below, above, and (approximately) at these critical fields is shown in Fig. 4.

At zero field both $\chi(T)$ and $C(T)$ drop exponentially with decreasing T at low temperatures due to the opening of the Haldane gap. In this case the ground state energy extrapolated from the internal energy $U(T)$ is -1.4015 , in agreement with the zero-temperature DMRG result.²⁵ The ground state excitation gap Δ can be determined from the temperature dependence of χ and C at low temperatures. If we adapt the ansatz that the low-lying excitation spectrum has approximately the form²⁶

$$\varepsilon(k) = \Delta + \frac{v^2}{2\Delta}(k - \pi)^2 + O(|k - \pi|^3), \quad (9)$$

where v is the spin wave velocity, it is then straightforward to show that, when $T \ll \Delta$, the spin susceptibility and the specific heat are

$$\chi(T) \approx \frac{1}{v} \sqrt{\frac{2\Delta}{\pi T}} e^{-\Delta/T}, \quad (10)$$

$$C(T) \approx \frac{3\Delta}{v\sqrt{2\pi}} \left(\frac{\Delta}{T}\right)^{3/2} e^{-\Delta/T}, \quad (11)$$

irrespective of the statistics of the excitations. Taking the ratio between $\chi(T)$ and $C(T)$ gives

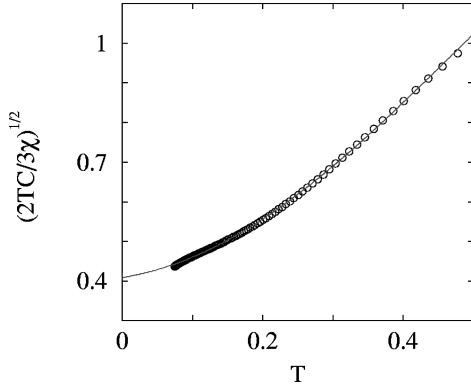


FIG. 5. $[2TC(T)/3\chi(T)]^{1/2}$ vs T for the $S=1$ Heisenberg model. ($m=100$ and $\tau=0.1$.)

$$\Delta = \lim_{T \rightarrow 0} \sqrt{\frac{2TC(T)}{3\chi(T)}}. \quad (12)$$

This is a very useful equation for determining Δ , especially from the point of view of experiments, since both $\chi(T)$ and $C(T)$ are experimentally measurable quantities.

Figure 5 shows $\sqrt{2TC(T)/3\chi(T)}$ as a function of T for the $S=1$ Heisenberg model at zero field. By extrapolation, we find that $\Delta \sim 0.41$ in agreement with the zero-temperature DMRG (Ref. 27) and exact diagonalization²⁸ results. Given Δ , the value of v can be found from Eq. (10) in the limit $T \rightarrow 0$. The value of v we found is ~ 2.45 , consistent with other numerical calculations.²⁶

At the two critical fields, $H_{c1} \sim 0.4105$ and $H_{c2} = 4$, both $\chi(T)$ and $C(T)/T$ diverge as $T^{-1/2}$ at low temperatures. This divergence, as for the $S=1/2$ case, is due to the square-root divergence of the density of states of the low-lying excitations. At H_{c1} , one branch of the $S=1$ excitations becomes massless and the low-energy excitation spectrum is approximately given by

$$\varepsilon(k) \sim \frac{v^2}{2\Delta} (k - \pi)^2. \quad (13)$$

If we assume that these excitations are fermionlike, i.e., satisfy the Fermi statistics (a short-range interacting Bose system is equivalent to a system of free fermions), then it is simple to show that when $T \ll \Delta$

$$\chi(T) \approx \frac{1}{3\pi v} \sqrt{\frac{2\Delta}{T}}, \quad (14)$$

$$C(T) \approx \frac{1}{2\pi v} \sqrt{2\Delta T}. \quad (15)$$

Thus in the limit $T \rightarrow 0$,

$$T^{1/2}\chi(T) = \frac{\sqrt{2\Delta}}{3\pi v} \sim 0.4, \quad (16)$$

$$T^{-1/2}C(T) = \frac{\sqrt{2\Delta}}{2\pi v} \sim 0.6. \quad (17)$$

By extrapolation, the TMRG result gives $T^{1/2}\chi|_{T \rightarrow 0} \sim 0.45$, which is close to that given by Eq. (16). The value of

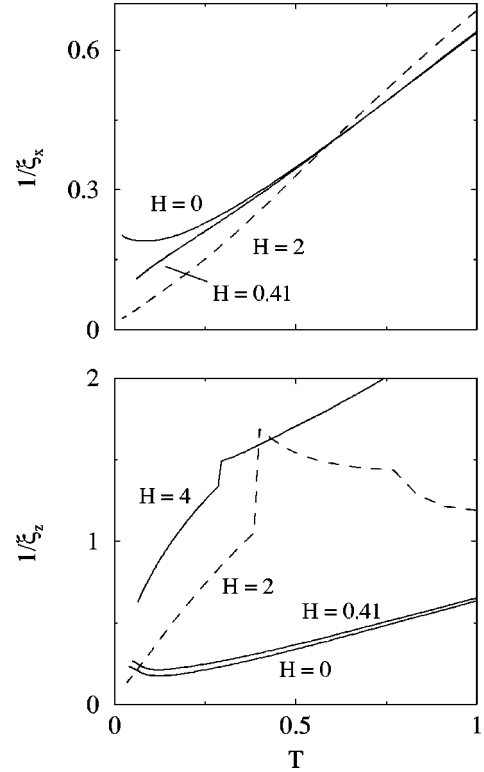


FIG. 6. (a) ξ_x^{-1} and (b) ξ_z^{-1} vs T for the spin-1 Heisenberg models. $\xi_x^{-1}(H=0)$ and $\xi_x^{-1}(H=0.4105)$ are almost indistinguishable when $T > 0.6$. $\tau=0.1$ and $m=100$ are used in the TMRG calculations.

$T^{-1/2}C|_{T \rightarrow 0}$ is difficult to determine accurately from the TMRG result since the error of $C(T)$ at low temperature is larger than $C(T)$ itself.

Figure 6 shows ξ_x^{-1} and ξ_z^{-1} of the $S=1$ model in different applied fields. Because of the Haldane gap, the longitudinal correlation length is finite even at zero field. Thus the longitudinal excitation mode is always full of gaps. Above H_{c1} but below H_{c2} , the transverse correlation length diverges at zero temperature. Thus the transverse mode is massless in this field regime. We note, however, that $\xi_{x,z}^{-1}$ at $H=0$ (similarly ξ_z^{-1} at $H=0.4105$) does not decrease monotonically at low temperatures, actually it starts to rise below a temperature T^* . This nonmonotonic behavior of ξ^{-1} at $H=0$ seems only due to the truncation error. Our preliminary calculation shows that T^* decreases with increasing m . But by far we still do not know if T^* is zero in the limit $m \rightarrow \infty$. Further investigation of the low-temperature behavior of ξ is needed. If we do an extrapolation using the TMRG data of ξ_x^{-1} above T^* , we find that $\xi_x(T=0) \sim 6.0$, which is consistent with the zero-temperature DMRG result.²⁵ If, however, the TMRG data below T^* are also included in the extrapolation, we find that $\xi_x(T=0)$ is only ~ 4.4 .

When $H > H_{c1}$, ξ_z^{-1} drops rather sharply at some temperatures. These sharp drops of ξ_z^{-1} happen when the second and third eigenvalues of the transfer matrix with $\sum_k \sigma^k = 0$ cross each other. The physical consequence of these sudden changes in the longitudinal correlation length is still unknown.

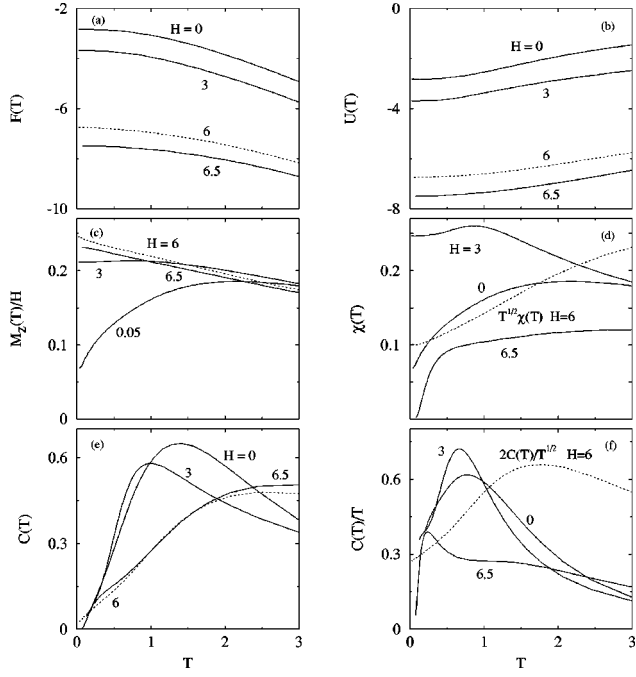


FIG. 7. Thermodynamic quantities for the spin-3/2 Heisenberg model in four applied fields, $H=0$ (or 0.05), 3, 6, and 6.5. When $H=6$, $T^{1/2}\chi(T)$ and $2C(T)/T^{1/2}$ (dotted lines) are shown in (d) and (f), respectively. $\tau=0.075$ and $m=81$ are used in the TMRG calculations.

C. $S=3/2$

The thermodynamic behaviors of the $S=3/2$ Heisenberg model, as shown in Fig. 7, are similar to those of the $S=1/2$ model. When $H < H_{c2}=6$, χ is always finite at zero temperature, indicating that the ground state is massless; above H_{c2} , the ground state is fully ferromagnetically polarized and a gap is open in the excitation spectrum; at H_{c2} , both $\chi(T)$ and C/T diverge as $T^{-1/2}$. At zero field, the susceptibility data, extrapolated to zero temperature, gives $\chi(0) \sim 0.67$, consistent with recent numerical calculations.^{8,11}

The crossover from quantum to classical behavior can be clearly seen (Fig. 8) by comparing the zero-field susceptibility and specific heat of the $S=1/2$, 1, and 3/2 spin chains with the corresponding results of the classical Heisenberg spin chain:³²

$$\chi(T) = \frac{1}{3T} \frac{1-u(T)}{1+u(T)}, \quad u(T) = \coth \frac{1}{T} - T, \quad (18)$$

$$C(T) = 1 - \frac{1}{T^2 \sinh^2(1/T)}. \quad (19)$$

At high temperatures, $T/S(S+1) > 1$, the quantum results approach asymptotically the classical ones. The agreement between the quantum and classical results persists down to progressively lower temperatures as S increases. At low temperatures, however, the difference between the results of the $S=3/2$ system and those of the classical model is still very large, indicating the importance of the quantum effects in the study of quantum spin chains. [Note for the classical Heisen-

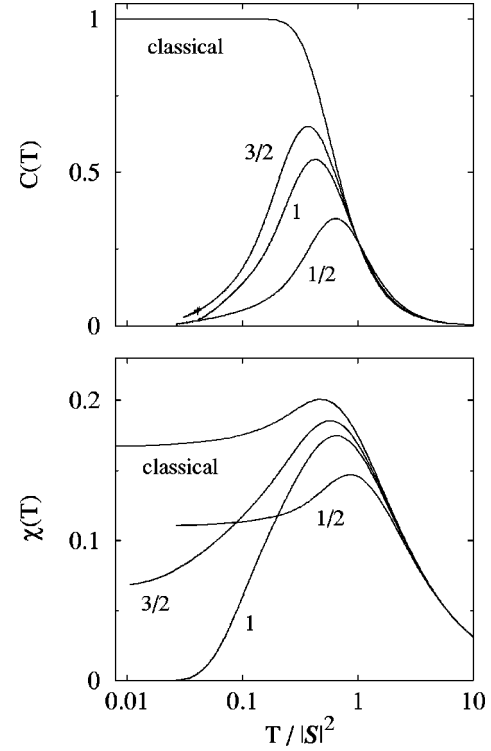


FIG. 8. The zero-field specific heat and susceptibility vs $T/|S|^2$ for the $S=1/2$, 1, and 3/2 spin chains [$|S|^2 = S(S+1)$]. The corresponding results for the classical Heisenberg model ($|S|^2=1$) are also shown for comparison.

berg model, $C(T)$ does not vanish at zero temperature. This is an unrealistic feature of this model.]

D. Zero-temperature magnetization

Figure 9 shows $M_z(T=0)$, extrapolated from the finite-temperature TMRG data of $M_z(T)$, for the $S=1/2$, 1, and 3/2 systems. For comparison the Bethe ansatz result²¹ for the $S=1/2$ Heisenberg model is also shown in the figure. With

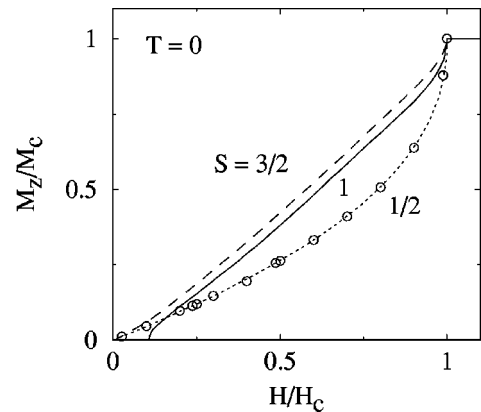


FIG. 9. Normalized zero-temperature magnetization M_z as a function of H/H_{c2} . The TMRG results for $S=1/2$ (circles), $S=1$ (solid line), and $S=3/2$ (dashed line) are obtained by extrapolation from the low- T values of M_z with $(m, \tau) = (81, 0.1)$, $(81, 0.1)$, and $(60, 0.75)$, respectively. Dotted line is the Bethe ansatz result for the $S=1/2$ system (Ref. 21).

increasing S , we found that M_z tends to approach its classical limit ($S \rightarrow \infty$) where M_z increases linearly with H , i.e., $M_z/S = H/H_{c2}$.

For the $S = 1/2$ system, the TMRG result agrees well with the Bethe ansatz one. A least squares fit to the curve of M_z up to the fourth order term of $\sqrt{H_{c2} - H}$ gives $M = M_c - a_1 \sqrt{H_{c2} - H} + a_2 (H_{c2} - H) - a_3 (H_{c2} - H)^{3/2} + a_4 (H_{c2} - H)^2$, with $a_1 \approx 0.448$, $a_2 \approx 0.123$, $a_3 = 0.05$, and $a_4 = 0.00744$. a_1 agrees very accurately with the exact value $\sqrt{2}/\pi$. In the weak-field limit, the asymptotic behavior of M_z is

$$M_z \approx \frac{H}{\pi^2} \left(1 - \frac{1}{2 \ln(H/H_{c2})} \right), \quad (20)$$

as predicted by the Bethe ansatz theory.^{29,30}

For the $S = 1$ model, $M_z(T=0)$ becomes finite when $H > H_{c1}$. In a very narrow regime of field near H_{c1} , $M_z(0)$ varies approximately as $\sqrt{H - H_{c1}}$, in agreement with the prediction of the Bose condensation theory.¹⁴ But the difference between the result of the Bose condensation theory

$$M_z(T=0) \approx \frac{\sqrt{2(H - H_{c1})\Delta}}{\pi v} \quad (21)$$

and that of the TMRG becomes already significant when $H - H_{c1} = 0.04$.

Near H_{c2} , M_z approaches its saturation value $M_c = S$ as a function of $\sqrt{H_{c2} - H}$ for the three spin systems we study. For the $S = 1/2$ and 1 systems, the TMRG results agree very accurately with the Bethe ansatz result^{29,31}

$$\frac{M_z}{S} = 1 - \frac{2}{\pi S} \sqrt{1 - \frac{H}{H_{c2}}}. \quad (22)$$

For the $S = 3/2$ system, the asymptotic regime of H is very narrow, and we cannot do a detailed comparison between the TMRG result and Eq. (22). The magnetization curve does not show a plateau at $M_z = 1/2$, in agreement with other studies.³³

E. Staggered susceptibility

To calculate the staggered susceptibility, we add a staggered magnetic field H_s to the Hamiltonian \hat{H} . The staggered magnetization is then calculated in a way similar to the calculation of the uniform magnetization. The staggered susceptibility χ_s is obtained by differentiating the staggered magnetization with respect to H_s . For half-odd-integer spin chains χ_s diverges as T^{-1} at low temperatures. Thus the staggered magnetization becomes saturated at low temperatures when $\chi_s(T)H_s > S$, since the maximum value of the staggered magnetization per spin is S . This means that to estimate accurately the zero-field staggered susceptibility the staggered field used should satisfy the condition $H_s \ll S/\chi_s(T_{\min})$, where T_{\min} is the lowest temperature to study.

Figure 10 shows the temperature dependence of χ_s for the $S = 1/2, 1$, and $3/2$ spin chains. At low temperatures, χ_s for the $S = 1/2$ model is expected to have the following asymptotic form

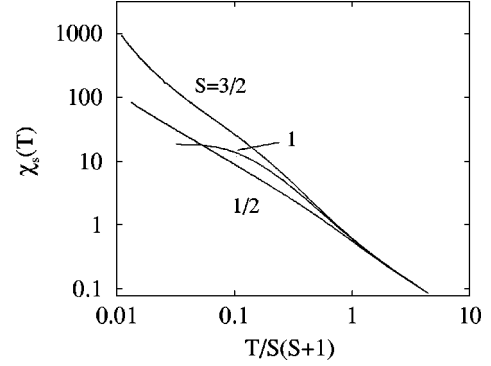


FIG. 10. The staggered susceptibility $\chi_s(T)$ at zero field. The parameters used for the $S = 1/2, 1$, and $3/2$ chains are $(H_s, \tau, m) = (0.0001, 0.1, 140)$, $(0.0001, 0.05, 100)$, and $(0.0001, 0.025, 81)$, respectively.

$$\chi_s = \frac{D_\chi}{T} \sqrt{\ln \frac{T_\chi}{T}} \quad (23)$$

according to a scaling argument.³⁴ Our TMRG result agrees well with this equation at low temperatures. By plotting $(T\chi_s)^2$ against $\ln T$, we find that $D_\chi \approx 0.30$ and $T_\chi \approx 10.5$, in agreement with a Monte Carlo calculation.⁸

For the $S = 1$ model, χ_s is finite at zero temperature. The extrapolated zero-temperature value of χ_s for the $S = 1$ model is 18.55, in agreement with other numerical calculations.^{8,35}

IV. CONCLUSION

In conclusion, the temperature dependence of the susceptibility, specific heat, and several other quantities of the quantum Heisenberg spin chains with spin ranging from $1/2$ to $3/2$ in a finite or zero applied magnetic field are studied using the TMRG method. At high temperatures, the quantum results for the specific heat as well as other thermodynamic quantities approach asymptotically the classical ones for both the integer and half-integer spin systems. At low temperatures, however, the quantum effect is strong and the integer spin chains behave very differently than the half-integer spin chains. For the $S = 1$ model, both χ and C decay exponentially at low temperatures due to the opening of the Haldane gap. For the $S = 1/2$ and $3/2$ spin chains, there is no gap in the excitation spectrum and both χ and C/T are finite at zero temperature. The thermodynamics of the Heisenberg spin chains in an applied field is mainly determined by the transverse excitation modes. At low temperatures, χ , C/T , and the transverse correlation length ξ_x diverge as $T^{-1/2}$ at H_{c2} for the $S = 1/2$ and $3/2$ models and at both H_{c1} and H_{c2} for the $S = 1$ model. This square-root divergence indicates that the low-energy spin excitations have a square-root divergent density of states at these critical fields. Our data agree well with the Bethe ansatz, quantum Monte Carlo, and other analytic or numerical results.

ACKNOWLEDGMENTS

I would like to thank R. J. Bursill, G. A. Gehring, S. J. Qin, and X. Wang for stimulating discussions.

- ¹F. D. M. Haldane, Phys. Lett. **93A**, 464 (1983).
- ²T. Nishino, J. Phys. Soc. Jpn. **64**, L3598 (1995).
- ³R. J. Bursill, T. Xiang, and G. A. Gehring, J. Phys.: Condens. Matter **8**, L583 (1996).
- ⁴X. Wang and T. Xiang, Phys. Rev. B **56**, 5061 (1997).
- ⁵In many compounds which mimic the behavior of spin chains, it has often been found that there are many other interactions between spins, apart from the isotropic exchange interaction. These interactions could be anisotropies [generally of the form $DS_{iz}^2 + E(S_{ix}^2 - S_{iy}^2)$ when S is larger than $1/2$], frustration, impurities, and interchain couplings. A TMRG study for the spin-1 Heisenberg model with single-ion anisotropy was published recently by D. Coombes, T. Xiang, and G. A. Gehring, J. Phys. Condens. Matter **10**, L159 (1998).
- ⁶H. Betsuyaku and T. Yokota, Prog. Theor. Phys. **75**, 808 (1986).
- ⁷S. Yamamoto and S. Miyashita, Phys. Rev. B **48**, 9528 (1993).
- ⁸Y. J. Kim, M. Greven, U. J. Wiese, and R. J. Birgeneau, cond-mat/9712257 (unpublished).
- ⁹V. A. Kashurnikov, N. V. Prokof'ev, B. V. Svistunov, and M. Troyer, cond-mat/9802294, Phys. Rev. B (to be published).
- ¹⁰R. Harayanan and R. R. P. Singh, Phys. Rev. B **42**, 10 305 (1990).
- ¹¹S. Moukouri and L. G. Caron, Phys. Rev. Lett. **77**, 4640 (1996).
- ¹²K. Katsumata *et al.*, Phys. Rev. Lett. **63**, 86 (1989).
- ¹³G. E. Granroth *et al.*, Phys. Rev. Lett. **77**, 1616 (1996).
- ¹⁴I. Affleck, Phys. Rev. B **43**, 3215 (1991).
- ¹⁵T. Koma, Prog. Theor. Phys. **81**, 783 (1989).
- ¹⁶D. C. Sorensen, SIAM J. Matrix Anal. Appl. **13**, 357 (1992).
- ¹⁷J. des Cloizeaux and J. J. Pearson, Phys. Rev. **128**, 2131 (1962).
- ¹⁸T. Yamada, Prog. Theor. Phys. **41**, 880 (1969); D. Fadeev and L. A. Takhtajan, Phys. Lett. **85A**, 375 (1981).
- ¹⁹J. C. Bonner and M. E. Fisher, Phys. Rev. **135**, A640 (1964).
- ²⁰I. Affleck, Phys. Rev. Lett. **56**, 746 (1986).
- ²¹R. B. Griffiths, Phys. Rev. **133**, A768 (1964).
- ²²S. Eggert, I. Affleck, and M. Takahashi, Phys. Rev. Lett. **73**, 332 (1994).
- ²³K. Nomura and M. Yamada, Phys. Rev. B **43**, 8217 (1991).
- ²⁴M. Takahashi, Phys. Rev. B **44**, 12 382 (1991).
- ²⁵S. R. White and D. A. Huse, Phys. Rev. B **48**, 3844 (1993).
- ²⁶E. S. Sorensen and I. Affleck, Phys. Rev. Lett. **71**, 1633 (1993).
- ²⁷S. R. White, Phys. Rev. Lett. **69**, 2863 (1992).
- ²⁸O. Golinelli, Th. Jolicœur, and R. Lacaze, Phys. Rev. B **50**, 3037 (1994).
- ²⁹C. N. Yang and C. P. Yang, Phys. Rev. **150**, 321 (1966); **150**, 327 (1966); **151**, 258 (1966).
- ³⁰H. M. Babujian, Nucl. Phys. B **215**, 317 (1983).
- ³¹J. B. Parkinson and J. C. Bonner, Phys. Rev. B **32**, 4703 (1985); R. P. Hodgson and J. B. Parkinson, J. Phys. C **18**, 6385 (1985).
- ³²M. E. Fisher, Am. J. Phys. **32**, 343 (1964).
- ³³M. Oshikawa, M. Yamanaka, and I. Affleck, Phys. Rev. Lett. **78**, 1984 (1997).
- ³⁴O. A. Starykh, R. R. P. Singh, and A. W. Sandvik, Phys. Rev. Lett. **78**, 539 (1997).
- ³⁵T. Sakai and M. Takahashi, Phys. Rev. B **42**, 1090 (1990).